



Spatiotemporal Nonlinear Dynamics in a Duffing-type System

Eduardo V. M. Reis¹, Marcelo A. Savi¹

¹Universidade Federal do Rio de Janeiro, COPPE - Department of Mechanical Engineering, Center for Nonlinear Mechanics

Abstract: This paper investigates the spatiotemporal nonlinear dynamics of a Duffing-type system. Conservative and non-conservative systems are treated showing complex spatiotemporal behaviors. Numerical simulations are carried out using finite difference method together with the fourth order Runge-Kutta method. A perturbation analysis is employed to understand nonlinear dynamics details, which allows the definition of different Lyapunov exponents. Different kinds of behaviors are discussed showing periodic, quasi-periodic and chaotic behaviors.

Keywords: Mechanical vibration, spatiotemporal chaos, pattern formation, Duffing.

INTRODUCTION

The study of spatiotemporal dynamics has become relevant throughout the years, being associated with scientific and technological problems, such as chemistry, fluid and solid mechanics (Reingruber and Holcman, 2009; Reis et al., 2018; Reis and Alves, 2021). These systems are related to challenging research topics, being related to rich behaviors associated with pattern formation and spatiotemporal chaos.

Pattern formation is a dynamical behavior of complex systems characterized by collective behavior built from individual or local dynamical behavior. Self-organization and dynamical characteristics are instances of patterns. Owolabi and Hammouch (2019) exploited different spatiotemporal patterns presented in Belousov-Zhabotinskii reaction systems. Biancalani et al. (2010) developed a stochastic version of the Brusselator model, observing Turing patterns within a specific parameter regions. Gotoda et al. (2015) analyzed the Kuramoto-Sivashinsky equation with an additional spatial derivative term standing for dispersion, showing that an exponential decay behavior of the power spectrum density at high frequencies is usually associated with spatiotemporal chaos.

Duffing-type systems are characterized by cubic nonlinearities, being able to model both electrical and mechanical systems (Savi and Pacheco, 2002; Kovacic and Brennan, 2011). Spatiotemporal characteristics can be investigated either by oscillator networks or partial differential equations (PDEs). Umberger et al. (1989) presented a pioneer study of a closed chain of Duffing oscillators. Musielak et al. (2005) studied routes to chaos in a network of Duffing oscillators showing that the increase of the number of degrees of freedom can lead to crisis, instead of period doubling, as the main route to chaos. Chatterjee et al. (2020) considered a network of Duffing oscillators subjected to harmonic excitation, calculating the convective Lyapunov exponents and observing the light-cone boundary during transient period. Reis and Savi (2022) studied a spatiotemporal conservative Duffing-type mechanical system governed by PDEs.

This paper investigates the spatiotemporal dynamics of a Duffing-type mechanical system governed by nonlinear partial differential equations with cubic nonlinearity. This system can represent several physical phenomena such as multiple connected Moon-Holmes beams (Moon and Holmes, 1979) or an acoustic metamaterial. Mathematical tools are defined, establishing an analysis of perturbed orbits in both space and time allowing different definitions to characterize spatiotemporal aspects: local, convective and mean perturbations. From perturbation analysis, it is possible to define local and mean Lyapunov exponents. Results show that periodic, quasi-periodic and chaotic responses can be obtained and that perturbation analysis is useful to characterize the spatiotemporal dynamics.

MATHEMATICAL MODEL

The spatiotemporal Duffing-type system is governed by a partial differential equation with cubic nonlinearity. Consider a dimensionless displacement u , spatial coordinate $x \in [0, 1]$ and time t . On this basis, the spatiotemporal dynamics is governed by the following dimensionless equation:

$$\ddot{u} = \sigma u'' + \sigma' u' - 2\xi \dot{u} + \frac{1}{2}(u - u^3) + \gamma \sin(\Omega t) \quad (1)$$

where $\dot{(\)}$ yields partial time derivative $\partial(\)/\partial t$, $(\)'$ yields spatial partial derivative $\partial(\)/\partial x$, $\sigma = \sigma(x)$ is a spatial coupling parameter, ξ is the dissipation coefficient, $\gamma = \gamma(x)$ is the excitation function and Ω is the excitation frequency. Systems with $\sigma' = 0$ are called reciprocal, being characterized by a spatial symmetrical energy propagation. On the other hand, $\sigma' \neq 0$ yields nonreciprocal systems, which are characterized by an asymmetrical energy propagation. Moreover, one should notice that the system with $\sigma = 0$ is spatially decoupled. Under this condition, the PDE turns into an ordinary

differential equations (ODE) that characterizes the Duffing oscillator. In this regard, the decoupled system has three equilibrium points: $u = -1$ (stable), $u = 1$ (stable), and $u = 0$ (unstable). Finally, the limit $\sigma \rightarrow \infty$ yields a rigid spatial attachment with only one possible solution: $u(x, t) = 0$. Dirichlet boundary conditions are assumed: $u(0, t) = u(1, t) = 0$.

PERTURBATION ANALYSIS

A dynamical system with spatial dependence can be generally written as follows: $\dot{\mathbf{u}} = f(\mathbf{x}, t, \mathbf{u}, \mathbf{u}', \mathbf{u}'', \mathbf{u}''', \dots, \mathbf{u}^{(m)}, \mathcal{P})$; where $\mathbf{u} = \mathbf{u}(\mathbf{x}, t) \in \mathbb{R}^n$ and \mathcal{P} represents a set of parameters. Let $\bar{\mathbf{u}}$ to be a reference solution of the equation of motion and its perturbation \mathbf{u}_p that can be obtained from a linearization of these equations: $\dot{\mathbf{u}}_p = D_{\mathbf{u}} f \mathbf{u}_p + \sum_{i=1}^m D_{\mathbf{u}^{(i)}} f \mathbf{u}_p^{(i)}$, where D is the Jacobian with respect to $\bar{\mathbf{u}}$. Therefore, the canonical form of the equations of motion and the perturbation equations for the Duffing-type system are given by

$$\begin{aligned} \dot{u} &= v \\ \dot{v} &= \sigma u'' + \sigma' u' - 2\xi v + \frac{1}{2}(u - u^3) + \gamma \sin(\Omega t) \\ \dot{u}_p &= v_p \\ \dot{v}_p &= \sigma u_p'' + \sigma' u_p' - 2\xi v_p + \frac{1}{2}(1 - 3u^2)u_p \end{aligned} \quad (2)$$

and boundary conditions yield $u(0, t) = u(1, t) = u_p(0, t) = u_p(1, t) = 0$.

The spatiotemporal dynamics can be characterized by the evolution of the perturbed orbits. A growing magnitude of \mathbf{u}_p , $|\mathbf{u}_p|$, yields a divergence from the reference orbit $\bar{\mathbf{u}}$, defining a chaotic response. On the other hand, a decrease of $|\mathbf{u}_p|$ yields a convergence between orbits, defining a periodic solution. For spatial extended systems, there are many efforts to define spatiotemporal dynamics, which includes spatiotemporal chaos (Cross and Hohenberg, 1993). In this manuscript, spatiotemporal dynamics is investigated using spatial and temporal perturbation characteristics, namely local perturbation quantity, ϕ , and an mean spatial quantity, ψ , which are defined as follows:

$$\begin{aligned} \phi(x, t) &= \sqrt{\mathbf{u}_p(\mathbf{x}, t) \cdot \mathbf{u}_p(\mathbf{x}, t)} = \sqrt{u_p(x, t)^2 + v_p(x, t)^2} \\ \psi(t) &= \sqrt{\frac{\int_V \phi(\mathbf{x}, t)^2 dV}{\int_V \phi(\mathbf{x}, 0)^2 dV}} = \sqrt{\frac{\int_0^1 u_p(x, t)^2 + v_p(x, t)^2 dx}{\int_0^1 u_p(x, 0)^2 + v_p(x, 0)^2 dx}} \end{aligned} \quad (3)$$

where \cdot represents the dot product and V is the volume of the spatial domain. A growing magnitude of both ϕ and ψ stands for the sensitivity of the dynamical response, which is an evidence of chaos. It should be pointed out that, for a spatial homogeneous evolution of ϕ , the quantity ψ becomes a relevant tool to characterize the spatial mean evolution of the local perturbation. The local Lyapunov exponent at a specific spatial position can be defined from the quantity ϕ , while the mean Lyapunov exponent can be estimated from the quantity ψ . On this basis, local and mean Lyapunov exponents are defined as follows,

$$\begin{aligned} \lambda_{\text{local}}(\mathbf{x}) &= \lim_{t \rightarrow \infty} \frac{1}{t} \log \left(\frac{\phi(\mathbf{x}, t)}{\phi(\mathbf{x}, 0)} \right) \\ \lambda_{\text{mean}} &= \lim_{t \rightarrow \infty} \frac{1}{t} \log \left(\frac{\psi(t)}{\psi(0)} \right) \end{aligned} \quad (4)$$

These quantities are employed to characterize different dynamical responses. The literature usually presents the Lyapunov spectrum as the main tool employed for evaluating extended systems, and a continuous set of positive exponents, given by the eigenvalues of the Jacobian matrix, are employed to define spatiotemporal chaos (Cross and Hohenberg, 1993; Pikovsky and Politi, 2016). Nevertheless, spatiotemporal responses can be complex being associated with multiple kinds of responses in different parts of space. Therefore, novel tools need to be employed to locally evaluate spatial dynamical response. On this basis, a local spatiotemporal chaos is defined for a specific region which presents $\lambda_{\text{local}}(x) > 0$ and irregular response in space. If $\lambda_{\text{local}}(x) > 0 \forall x$ and the full domain presents an irregular configuration, the response is defined as full spatiotemporal chaos and λ_{mean} can be employed to quantify this behavior. Following this idea, a local (full) periodic response is defined when if $\lambda_{\text{local}}(x) \leq 0 (\forall x)$ and a closed orbit in the state space. Finally, a local (full) quasi-periodic response is defined when $\lambda_{\text{local}}(x) = 0 (\forall x)$ and a torus-like orbit in state space.

NUMERICAL SIMULATIONS

This section discusses different types of spatiotemporal dynamical responses observed in the Duffing-type system. All simulations are carried out considering a reciprocal system with $\sigma = 5 \times 10^{-4}$ by considering the fourth order finite

difference scheme for spatial discretization with 5001 points and the fourth order Runge-Kutta method with a time step of 5×10^{-4} for time discretization.

Initially, a conservative Hamiltonian system is considered, which means that $\xi = \gamma = 0$ and the mechanical energy is conserved. On this basis, different values of h , defined as the amount of mechanical energy, are of concern. Initial conditions consider $v(x, 0) = 0$ and $u(x, 0) = \chi \sin(\pi x)$, where χ is a coefficient standing for the amplitude. A space-time split is employed to evaluated separately temporal and spatial aspects of the dynamical behavior. First, the response is evaluated at a specific space position, namely $x = 0.5$. Fig. 1 shows the time history and its respective frequency domain analysis. Frequency domain is obtained using a Fast Fourier Transformation (FFT), which maps $(t, u(x = 0.5)) \rightarrow (\omega, A)$. One observes complex and irregular responses in time for both mechanical energy levels. In frequency domain, the response is spread over several frequencies. It should also be pointed out that, for $h = 0.5$, the response is an intra-well oscillation, occurring around only one well of the Duffing-type potential energy. For $h = 5$, the mechanical energy level is higher and the system has enough energy to overcome the well energy barrier, presenting an inter-well oscillation, which occurs around both wells.

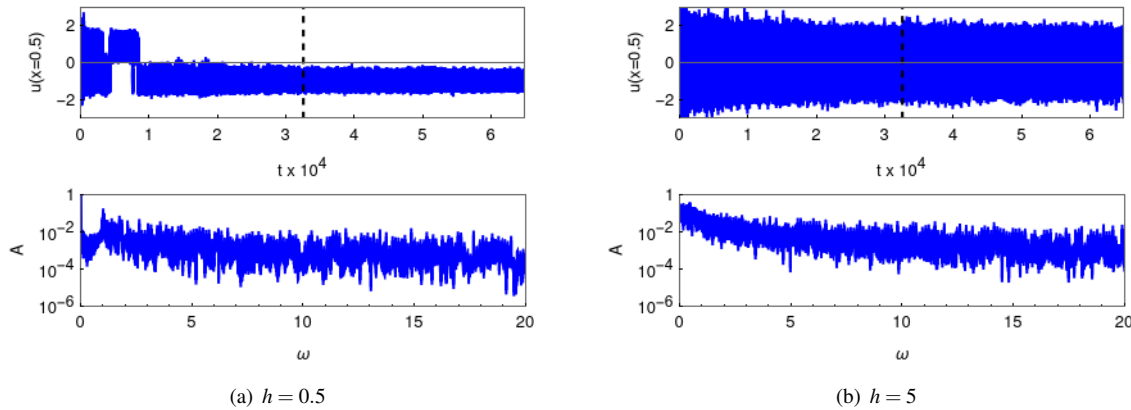


Figure 1 – Displacement at $x = 0.5$ over time and frequency domains for two h values. The red lines stand for $t = 325 \times 10^2$, where the spatial analysis is performed.

Spatial analysis is performed by considering the spatial distributed displacement at a fixed time: $t = 325 \times 10^2$. Fig. 2 shows the spatial configuration in space and spatial frequency domain for both $h = 0.5$ and $h = 5$. One observes an irregular spatial configurations for both energy levels. The spatial frequency domain analysis is employed also using a FFT that transformed $(x, u(t = 325 \times 10^2)) \rightarrow (\lambda, \Lambda)$.

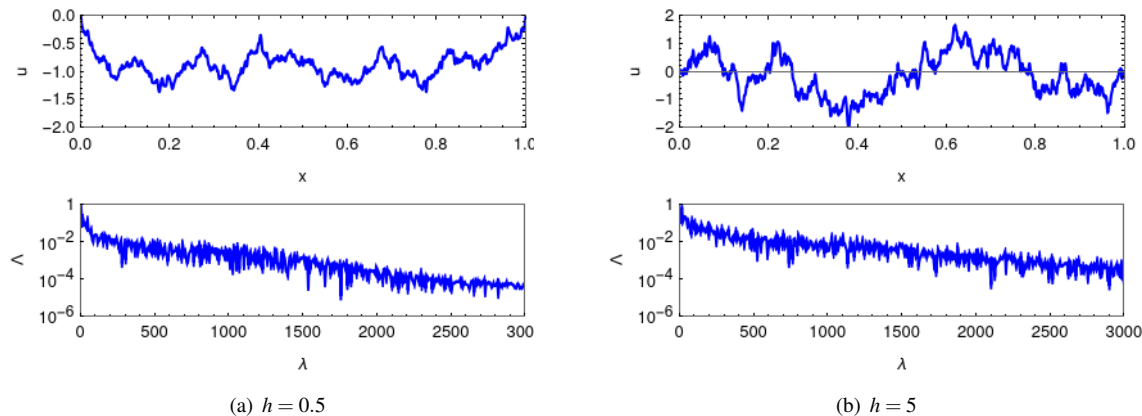


Figure 2 – Displacement at $t = 325 \times 10^2$ over space and spatial frequency domains.

Since the displacement in both temporal and spatial analysis are irregular, it suggests spatiotemporal chaos. The evolution in the space-time map of an initial bell shaped perturbation is evaluated and depicted in Fig. 3. The initial condition for the perturbation is given by the Gaussian $u_p(x, 0) = 2.825 \exp[-100(x - 0.5)^2]$ and $v_p(x, 0) = 0$. One can observe that, as time evolves, the bell shaped perturbation is distorted and spreads in space. The dashed lines stand for the evolution of the perturbation boundary is defined as the outer isoline with $\phi = 10^{-1}$. Also, the local perturbation growth rate is approximately uniformly in space and exponentially in time.

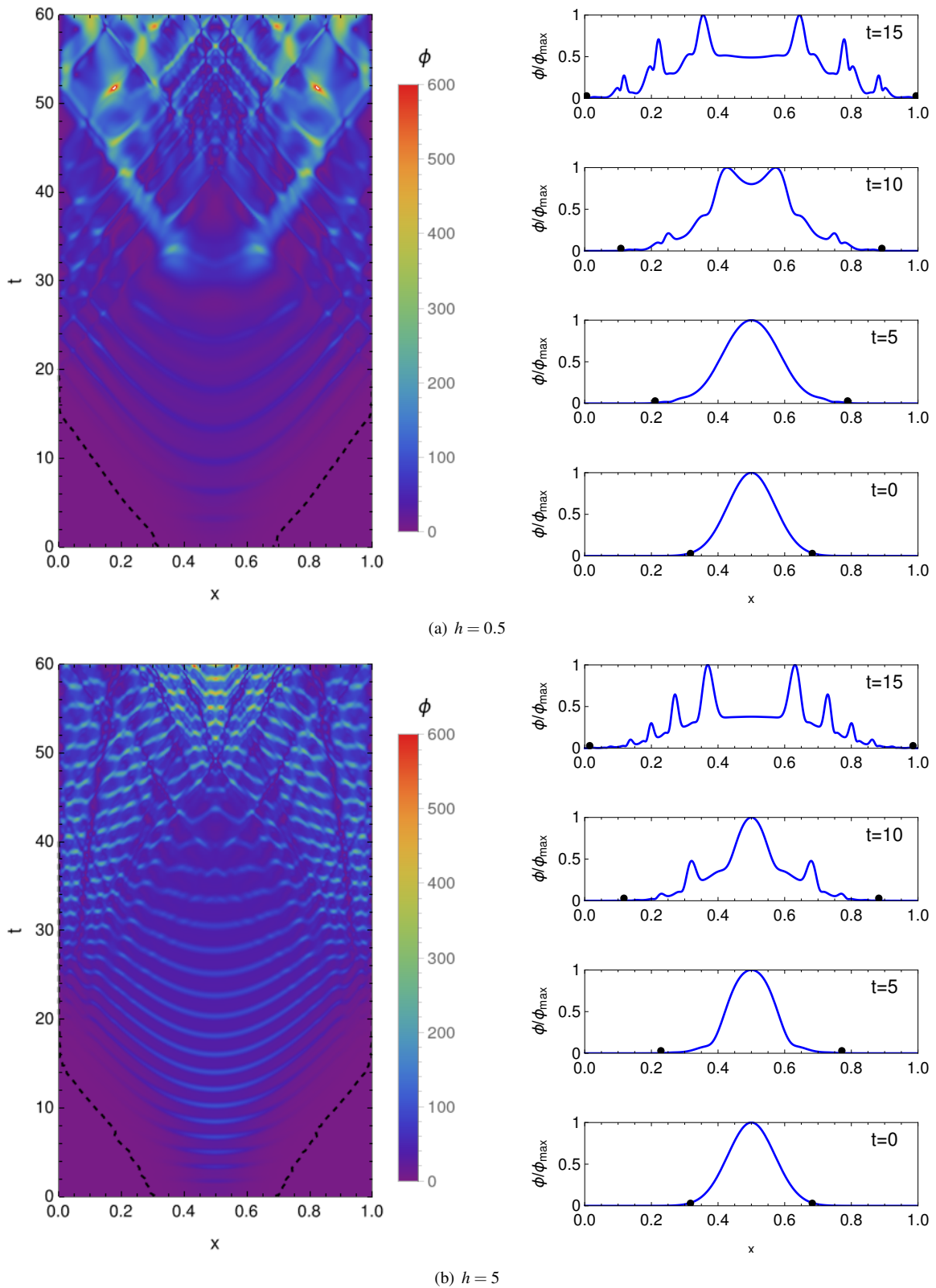


Figure 3 – Space-time map showing the evolution and spread of the local perturbation ϕ (left) and its normalized configuration at discrete initial times (right). Boundaries of the perturbation are highlighted by dashed black line in the left column and as black dots on the right column.

Due to this uniform evolution of the local perturbation in space, one can employ the λ_{mean} to quantify the perturbation mean spatial perturbation growth rate. Fig. 4 presents λ_{mean} for several values of mechanical energy of the system. It shows λ_{mean} is strictly positive, characterizing spatiotemporal chaos, and increases as h grows. At $h \gtrsim 3$, it reaches a plateau. This occurs because when $h \gtrsim 3$, oscillation of most of the spatial domain is inter-well, while $h \lesssim 3$ oscillation

is predominant intra-well.

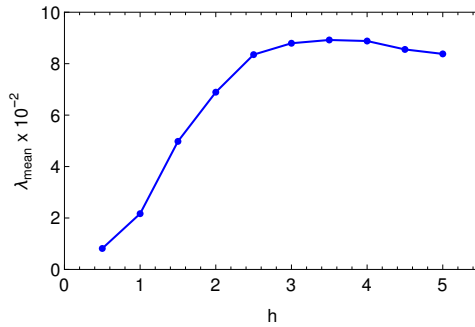


Figure 4 – Mean Lyapunov exponent for the conservative system.

A non-conservative case is now in focus assuming $\xi = 5 \times 10^{-3}$, $\Omega = 8$ and a nonuniform excitation function: $\gamma(x) = \frac{B}{2} \tanh(40x - 20) + \frac{1}{2}$, where B is a constant standing for the excitation amplitude. In this regard, the first half of the spatial domain is subjected to a small excitation amplitude whilst the other half is subjected to a larger excitation. One should notice that $P = 2\pi/\Omega$ is the excitation period. Initial conditions are assumed to be $u(x, 0) = v(x, 0) = 0$. Different responses are found for different values of B : periodic, quasi-periodic and spatiotemporal chaos. The identification is done by a space-time split analysis and monitoring the local Lyapunov exponent.

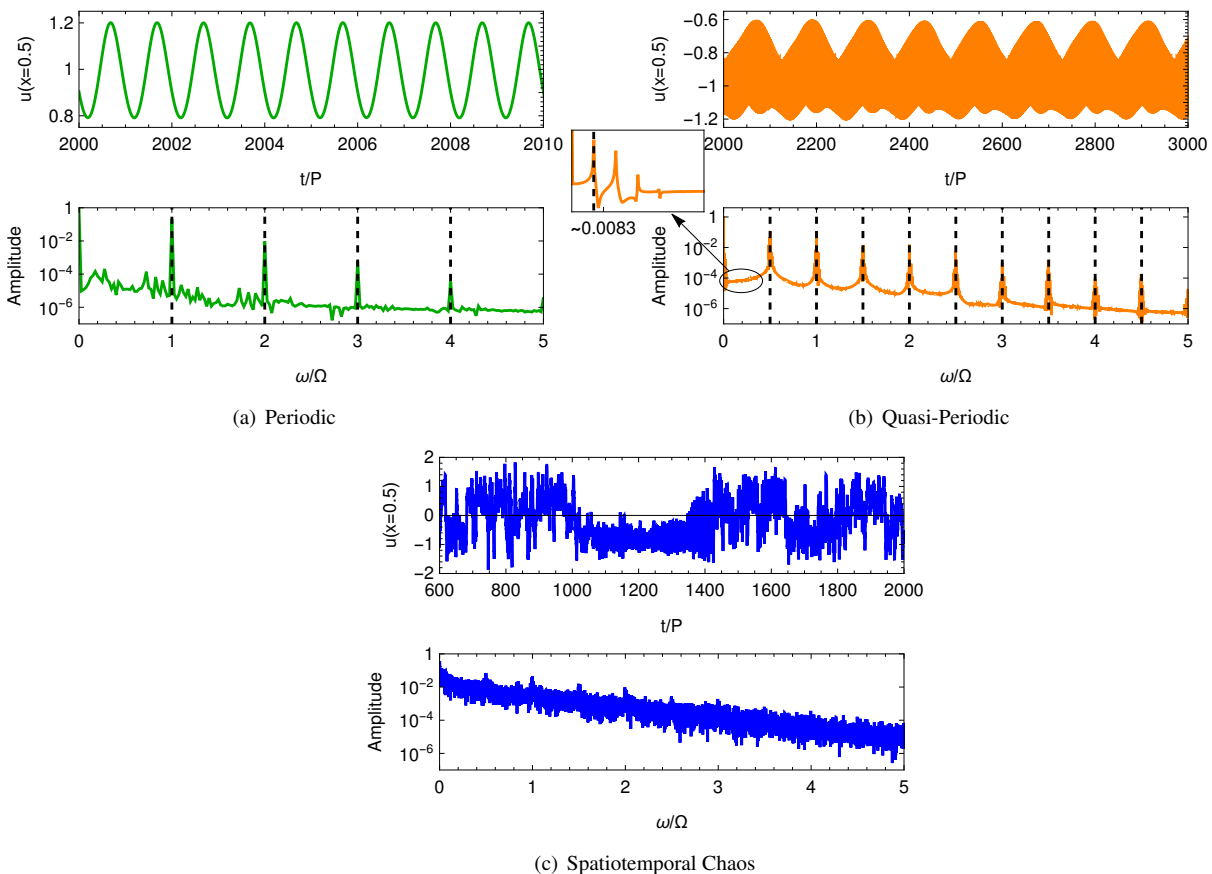


Figure 5 – Displacement at $x = 0.5$ over time and frequency domains for different kinds of dynamical response: (a) Periodic with $B = 5$, (b) Quasi-periodic with $B = 10$ and (c) Spatiotemporal chaotic with $B = 20$.

Fig. 5 depicts the displacement time history and frequency domains at $x = 0.5$. Note that it is possible to identify the signatures of each type of dynamical response. Periodic response presents a time history that shows a pattern that is repeated over time, oscillating around $u \approx 1$, which is a stable equilibrium point for the decoupled system ($\sigma = 0$). The response in frequency domain is regular, being characterized by the excitation frequency and its harmonics. A quasi-periodic response is characterized by the presence of discrete peaks in the frequency spectrum which are incommensurate.

For this type of response, one observes harmonics and sub-harmonics of the excitation frequency that are incommensurate with another peak observed at $\omega/\Omega \approx 0.0083$. Finally, the chaotic response is characterized by an irregular regime in both time and frequency domains. It is worthwhile mentioning that, besides the excitation function is not spatially homogeneous, the local Lyapunov distribution is homogeneous. In this regard, the mean Lyapunov exponent can be employed to characterize these three different responses, yielding: $\lambda_{\text{mean}} = -0.0044$ for the periodic response, $\lambda_{\text{mean}} = 0$ for the quasi-periodic, and $\lambda_{\text{mean}} = 0.051$ for the spatiotemporal chaotic response.

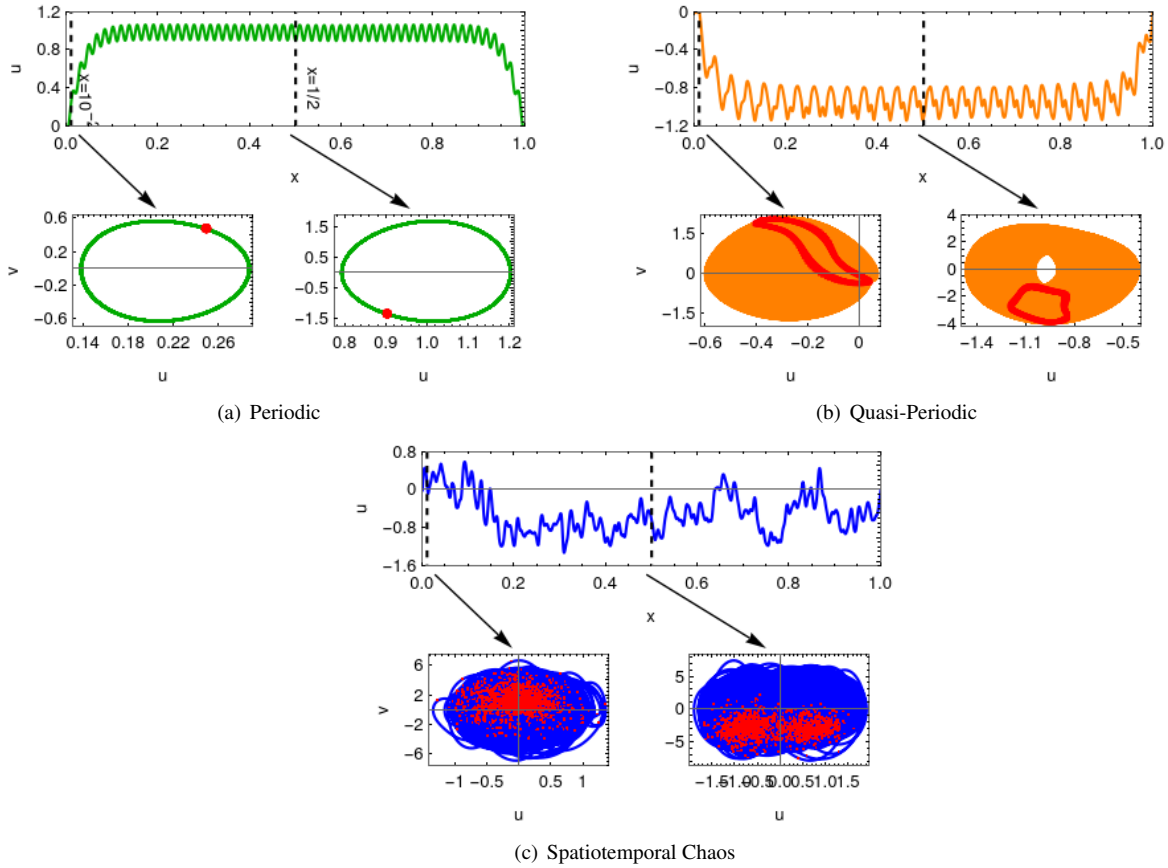


Figure 6 – Spatial configuration and state space at $x = 10^{-2}$ and 0.5 for different kinds of dynamical response with $\Omega = 8$: (a) periodic response with $B = 5$; (b) quasi-periodic with $B = 10$; (c) spatiotemporal chaos with $B = 20$.

The displacement in space is now of concern. Fig. 6 shows the spatial configurations at $t = 2000P$ and the state space with Poincaré sections at $x = 10^{-2}$ and 0.5 obtained in the range $2000P \leq t \leq 3000P$. Poincaré sections are obtained with a time interval of $1P$. One observes the periodic response that presents a symmetric pattern with respect to $x = 0.5$, although the excitation function is not spatially symmetric. Therefore, the symmetry is achieved due to energy propagation effect from spatial coupling. State space is characterized by a closed orbit with period $1P$, in accordance with the temporal analysis showed in Fig. 5. Moreover, both displacement and velocity amplitudes are lower at the position closer to the boundary ($x = 10^{-2}$), which is also expected due to the Dirichlet boundary condition $u(0, t) = u(1, t) = 0$. For the quasi-periodic response, one observes a quasi-symmetric spatial pattern, and Poincaré sections are characterized by an almost closed curve. Finally, the spatiotemporal chaos yields an irregular regime in space, and Poincaré sections do not show clearly a strange attractor due to the high dimension of the system.

CONCLUSIONS

This paper deals with an investigation of the spatiotemporal dynamics of a continuous Duffing-type system governed by a partial differential equation with cubic nonlinearity. Conservative and non-conservative cases are treated. A perturbation analysis is developed allowing the definition of local and mean perturbation quantities, which can be further employed for estimating local and mean Lyapunov exponents. These are important tools to characterize spatiotemporal dynamics. Results show irregular responses in both time and space in the conservative system, being associated with positive Lyapunov exponents, which indicates spatiotemporal chaos. The non-conservative system, on the other hand, generates three different responses: periodic, quasi-periodic and spatiotemporal chaos. These responses are identified employing space-time split, state space analyses and local Lyapunov exponent.

ACKNOWLEDGMENTS

The authors would like to acknowledge the support of the Brazilian Research funding Agencies FAPERJ, CAPES and CNPq.

REFERENCES

- Biancalani, T., Fanelli, D. and Di Patti, F., 2010, "Stochastic Turing patterns in the Brusselator model", *Physical Review E*, Vol.81
- Chatterjee, A.K., Kundu, A. and Kulkarni, M., 2020, "Spatiotemporal spread of perturbations in a driven dissipative Duffing chain: An out-of-time-ordered correlator approach", *Physical Review E*, Vol.102
- Cross, M. and Hohenberg, P., 1993, "Pattern formation outside of equilibrium", *Reviews of modern physics*, Vol. 65
- Gotoda, H., Pradas, M. and Kalliadasis, S., 2015, "Nonlinear forecasting of the generalized kuramoto-sivashinsky equation", *International Journal of Bifurcation and Chaos*, Vol.25, pp. 1-19
- Kovacic, I. and Brennan, M.J, 2011, "The Duffing equation: nonlinear oscillators and their behaviour", John Wiley & Sons
- Moon, F.C. and Holmes, P.J., 1979, "A magnetoelastic strange attractor", *Journal of Sound and Vibration*, Vol.65, pp. 275-296
- Musielak, D.E., Musielak, Z.E. and Benner, J.W., 2005, "Chaos and routes to chaos in coupled Duffing oscillators with multiple degrees of freedom", *Chaos, Solitons & Fractals*, Vol.24, pp. 907-922
- Owolabi, K.M and Hammouch, Z., 2019, "Spatiotemporal patterns in the Belousov–Zhabotinskii reaction systems with Atangana-Baleanu fractional order derivative", *Physica A: Statistical Mechanics and its Applications*, Vol.523, pp. 1072-1090
- Pikovsky, A. and Politi, A., "Lyapunov exponents: a tool to explore complex dynamics", Cambridge University Press, 2016
- Reingruber, J. and Holcman, D., 2009, "Diffusion in narrow domains and application to phototransduction", *Physical Review E - Statistical, Nonlinear, and Soft Matter Physics*, Vol.79, pp. 1-4
- Reis, E.V.M., Sphaier, L.A., Nunes, L.C.S. and Alves, L.S de B., 2018, "Dynamic response of free span pipelines via linear and nonlinear stability analyses", *Ocean Engineering*, Vol. 163, pp. 533-543
- Reis, E.V.M. and Alves, L.S. de B., 2021, "Convective and Absolute Instabilities Induced by Viscous Dissipation in the Thermocapillary Convection With Through-Flow", *Journal of Heat Transfer*, Vol. 143
- Reis, E.V.M. and Savi, M.A, 2022, "Spatiotemporal chaos in a conservative Duffing-type system", *Chaos, Solitons & Fractals*, Vol. 165
- Savi, M.A. and Pacheco, P.M.C.L., 2002, "Chaos in a two-degree of freedom Duffing oscillator", *Journal of the Brazilian Society of Mechanical Sciences*, Vol.24, pp. 115-121
- Umberger, D.K., Grebogi, C., Ott, E. and Afeyan, B., 1989, "Spatiotemporal dynamics in a dispersively coupled chain of nonlinear oscillator", *Physical Review A*, Vol.39, pp. 4835-4842

RESPONSIBILITY NOTICE

The author(s) is (are) the only responsible for the printed material included in this paper.